Breakdown of the Giant Spin Model in the Magnetic Relaxation of the Mn6 Nanomagnets

Breakdown of the Giant Spin Model in the Magnetic Relaxation of the Mn_6 Nanomagnets

S. Carretta,[1] T. Guidi,[2] P. Santini,[1] G. Amoretti,[1] O. Pieper,[2,3] B. Lake,[2,3] J. van Slageren,[4,5] F. El Hallak,[4] W. Wernsdorfer,[6] H. Mutka,[7] M. Russina,[2] C. J. Milios,[8] and E. K. Brechin[8]

[1]*Dipartimento di Fisica, Università di Parma, I-43100 Parma, Italy*
[2]*Hahn-Meitner Institut, Glienicker Strasse 100, 14109 Berlin, Germany*
[3]*Institut für Festkörperphysik, Technische Universität Berlin, 10623 Berlin, Germany*
[4]*1. Physikalisches Institut, Universität Stuttgart, D-70550 Stuttgart, Germany*
[5]*School of Chemistry, University of Nottingham, Nottingham NG7 2RD, United Kingdom*
[6]*Laboratoire Louis Néel-CNRS, F-38042 Grenoble Cedex, France*
[7]*Institute Laue-Langevin, B.P. 156, F-38042 Grenoble Cedex, France*
[8]*University of Edinburgh, West Mains Road, Edinburgh, EH9 3JJ, United Kingdom*

(Received 28 November 2007; published 16 April 2008)

We study the spin dynamics in two variants of the high-anisotropy Mn_6 nanomagnet by inelastic neutron scattering, magnetic resonance spectroscopy and magnetometry. We show that a giant-spin picture is completely inadequate for these systems and that excited S multiplets play a key role in determining the effective energy barrier for the magnetization reversal. Moreover, we demonstrate the occurrence of tunneling processes involving pair of states having different total spin.

DOI: 10.1103/PhysRevLett.100.157203 PACS numbers: 75.50.Xx, 75.40.Gb, 75.60.Jk, 78.70.Nx

A class of magnetic molecules which has recently attracted considerable interest is that of the so-called molecular nanomagnets (MNMs), which at low temperature T display slow relaxation of the magnetization of molecular origin [1]. The interest in MNMs has been primarily driven by the envisaged possibility of exploiting their single-molecule magnetic bistability for high-density information storage. In addition, MNMs constitute model systems for investigating quantum phenomena like quantum tunneling of the magnetization M [1,2]. For $T \gtrsim 1$ K, magnetic relaxation is driven by interactions of the spin degrees of freedom with phonons, and it is usually modeled by considering only the ground total spin multiplet, thus describing each MNM as a giant-spin S in an effective easy-axis (double-well) potential. The reversal of the giant spin occurs through a multistep Orbach process in which the square modulus $S(S+1)$ is conserved. This model results in a thermally activated behavior for the relaxation time, $\tau = \tau_0 \exp(U/k_B T)$, where U is set by the axial anisotropy felt by the giant spin. In addition, for specific values of the applied magnetic field the giant spin undergoes resonant tunneling processes which lead to a marked decrease of τ. The giant-spin approach has been successfully used to interpret the experimental relaxation data of several nanomagnets (e.g., [3,4]). Recently, it has been shown that mixing of the wave functions of high-energy S manifolds with those of the ground manifold (S mixing), even if small enough to be immaterial in the thermally-activated relaxation regime, crucially affects quantum tunneling of M in MNMs by strongly renormalizing the tunneling gap [5–7]. A different and still open important issue is how thermal relaxation in a MNM is affected by the presence of excited S-multiplets at energies smaller than the barrier U. Such states could provide intermultiplet relaxation and tunneling pathways, leading to a breakdown of the giant-spin paradigm and to new richer physical properties.

In this Letter, we demonstrate that excited S-multiplets may strongly influence the energy barrier for the reversal of M in nanomagnets. We exploit inelastic neutron scattering (INS) and frequency domain magnetic resonance spectroscopy (FDMRS) to investigate two variants of a Mn_6 ($S = 12$) molecule having very similar structures but very different energy barriers (a record barrier $U = 86.4$ K, and $U = 53.1$ K [8,9], see Fig. 1) and we calculate the spectrum of

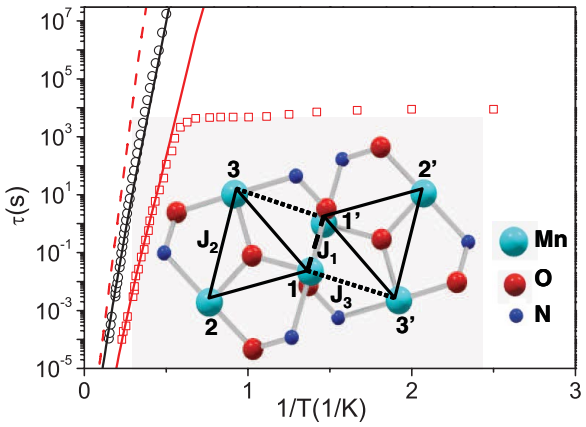

FIG. 1 (color online). T dependence of the leading relaxation time τ. Circles and squares are experimental data of (i) [8] and (ii) [9], respectively. In the thermally activated regime, $\tau \simeq \tau_0 \exp(U/k_B T)$ with $U \simeq 86.4$ K, $\tau_0 \simeq 2 \times 10^{-10}$ sec for (i), and $U \simeq 53.1$ K, $\tau_0 \simeq 8 \times 10^{-10}$ sec for (ii). Continuous lines are the present theoretical calculations. The dashed line is the result of the calculation for (ii) when excited multiplets are neglected. Inset: structure of the Mn_6 core. H and C ions are omitted for clarity.

relaxation times. We show that the large decrease in U is not the result of a smaller anisotropy but is mainly due to the activation of efficient relaxation paths passing through excited S multiplets partially nested within the ground one. In addition, we demonstrate that because of S-mixing in the wave functions these nested excited manifolds lead to resonant intermultiplet tunneling processes for fields of a few thousands of Gauss. These produce additional steps in hysteresis cycles which could not be explained by the giant-spin model.

The two investigated Mn_6 complexes of chemical formula $Mn_6O_2(Et\text{-}sao)_6(O_2CPh(Me)_2)_2(EtOH)_6$ (i) and $Mn_6O_2(Et\text{-}sao)_6(O_2CPh)_2(EtOH)_4(H_2O)_2$ (ii) are isostructural and have a magnetic core consisting of six Mn^{3+} ions arranged on two triangles bridged by oxygen atoms (inset of Fig. 1). Each Mn^{3+} ion has a distorted octahedral cage of ligands, with the Jahn-Teller axes all approximately perpendicular to the planes of the triangles. The six Mn^{3+} ions have spin $s = 2$ and are coupled by dominant ferromagnetic interactions, leading to a high $S = 12$ total spin ground state, as determined by magnetization measurements [8,9]. In spite of the very similar structure of the two molecules, combined ac susceptibility and dc relaxation measurements provide very different results for the effective energy barriers.

All measurements can be reproduced by describing each Mn_6 molecule by the following Hamiltonian

$$H = \sum_{i<j} J_{ij}\mathbf{s}(i)\cdot\mathbf{s}(j) + \sum_i d_i s_z^2(i) + \sum_i e_i[s_x^2(i) - s_y^2(i)] + \sum_i c_i[35s_z^4(i) + [25 - 30s(s+1)]s_z^2(i)] + g\mu_B\mathbf{B}\cdot\mathbf{S}, \quad (1)$$

where $\mathbf{s}(i)$ are spin operators of the ith Mn ion and $\mathbf{S} = \sum_i \mathbf{s}(i)$ is the total spin. The first term is the isotropic exchange, while the second, third and fourth terms describe local crystal-fields (a z axis perpendicular to the triangles plane is assumed) and $\mathbf{B}$ is the external field [1]. The structure of Mn_6 fixes the minimal number of free parameters in (1): three different exchange constants J_1, J_2, J_3 (Fig. 1) and two sets of crystal-field (CF) parameters d_1, c_1, e_1 and d_2, c_2, e_2. Indeed, sites 1 and 1′, 2 and 2′, 3 and 3′ are related by an inversion center. The ligand cages of sites 1 and 3 are rather similar and we assumed them to be equal. The dominant CF terms are the second-order axial ones. Since experimental information is insufficient to fix the four small c and e parameters,we have chosen to constrain the ratios c_1/c_2 and e_1/e_2 to the ratio d_1/d_2. The anisotropic terms break rotational invariance and here lead to a large amount of mixing of different S multiplets (S mixing [5]).

To determine the parameters appearing in (1), we have performed INS experiments using the time-of-fight spectrometers NEAT at the Hahn-Meitner Institut (Berlin) and IN5 at the Institute Laue-Langevin (Grenoble) and FDMRS measurements at the University of Stuttgart.

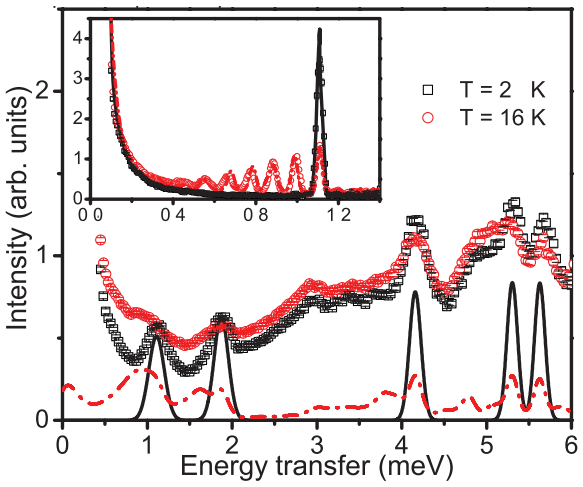

FIG. 2 (color online). INS spectra collected for (i) on IN5 with incident wavelength of 3.4 Å and 6.7 Å (inset) for $T = 2$ K (black) and $T = 16$ K (red). Lines are theoretical calculations.

Nondeuterated polycrystalline samples have been used. Figure 2 shows some INS data for compound (i). At $T = 2$ K only the ground state ($|S = 12, M = \pm 12\rangle$) is populated and due to the INS selection rules the most intense transitions are those to $|S = 12, M = \pm 11\rangle$ observed at 1.1 meV and to the five doublets $|S = 11, M = \pm 11\rangle$ of which four were observed at 1.9, 4.2, 5.3, and 5.6 meV (see Fig. 2) [10]. The magnetic origin of these excitations is confirmed by their form-factor and by the fact that their intensity decreases as the sample is heated up, whereas the features around 3.5 meV are due to phonons and are present in both variants [11]. To investigate the splitting of the ground manifold, higher resolution experiments have been performed (Fig. 2 inset) with T up to 16 K. Because of the sizeable uniaxial distortion of the octahedral cages around Mn ions, quite large d_i are expected. Hence, a simultaneous fit of exchange and CF interactions has to be performed. The results are summarized in Table I and the corresponding calculated INS spectra are reported in Fig. 2. Exchange is predominantly ferromagnetic and the strongest exchange interaction is the intertriangle one between the two central Mn ions. Nonaxial contributions to H appear to be $\lesssim 1\%$ of the axial ones but too small to be determined precisely by these measurements. The assignment of the observed peaks to intramultiplet or intermultiplet transitions has been confirmed by the comparison with FDMRS results where intense transitions occur only between states whose dominant components have the same

TABLE I. Exchange and dominant CF parameters for Eq. (1) (in meV) deduced by fitting INS and FDMRS data.

	J_1	J_2	J_3	d_1	d_2	c_1
(i)	−0.84(5)	−0.59(3)	0.01(1)	−0.20(1)	−0.76(2)	−0.0010(3)
(ii)	−0.61(5)	−0.31(2)	0.07(2)	−0.23(1)	−0.97(5)	−0.0008(3)

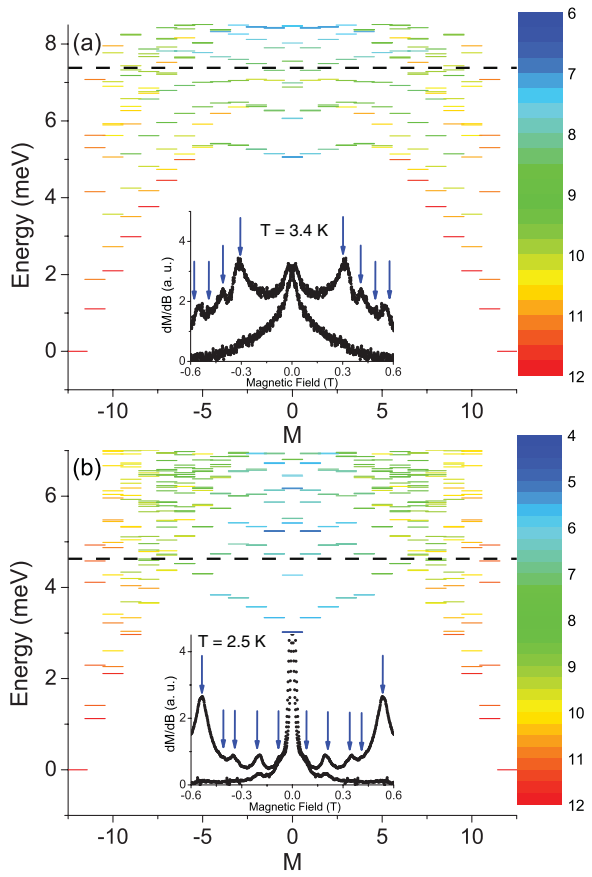

FIG. 3 (color). Energy levels as a function of the z-component of the total spin for (i) (a) and (ii) (b). The color maps S_{eff}, where $<S^2> := S_{\text{eff}}(S_{\text{eff}} + 1)$. The black dashed lines correspond to the observed value of U. Insets: examples of derivative of the hysteresis curves measured in [8,9] showing the presence of tunneling peaks absent in a giant-spin model. For each value of B, there are two points corresponding to increasing or decreasing B in the hysteresis cycle. Arrows indicate the calculated (anti-)crossing positions.

total spin. Ferromagnetic exchange couplings have the same order of magnitude as the axial CF interactions. This makes Mn_6 unique, as several excited multiplets are partially nested within the ground $S = 12$ one [see Fig. 3(a)]. For instance, a multiplet with easy-plane effective anisotropy is clearly visible around 5 meV, well below the anisotropy barrier of the $S = 12$ ground multiplet (~ 6.8 meV). This nesting leads to a very large degree of S mixing of the spin wave functions and strongly influences the relaxation behavior (see below).

Analogous investigations have been performed on variant (ii). By measuring with an incident wavelength of 3.4 Å on IN5 at $T = 2$ K, we have accessed the whole set of transitions allowed by the INS selection rules (Fig. 4). The intramultiplet transition from the $|S = 12, M_S = \pm 12\rangle$ ground state to the $|S = 12, M_S = \pm 11\rangle$ first-excited level is at about the same energy as in variant (i), i.e. $\sim$1.1 meV. This indicates that the effective anisotropy of the ground $S = 12$ multiplet is similar in (i) and (ii). In

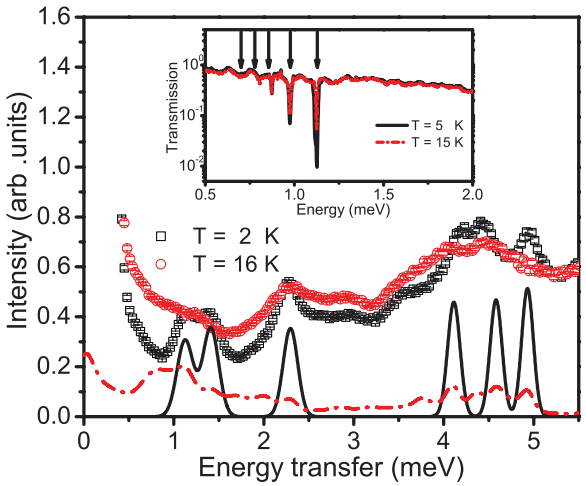

FIG. 4 (color online). (a) INS spectra collected for (ii) on IN5 with incident wavelength of 3.4 Å for $T = 2$ and 16 K. Lines are theoretical calculations. Inset: FDMRS spectra at 5 and 15 K. Arrows indicate the calculated transition energies.

contrast, the energies of the intermultiplet $S = 12 \rightarrow S = 11$ excitations considerably decrease in (ii). This provides direct evidence of a substantial decrease of isotropic exchange which leads to an even larger degree of nesting of excited S multiplets within the ground one. Figure 4 reports the energy dependence of the FDMRS transmission signal. The five dips are of magnetic origin and all but one correspond to transitions within the $S = 12$ multiplet (the dip near 0.8 meV corresponds to an $S = 11$ intramultiplet transition). Arrows indicate the positions of the transitions calculated with the parameters reported in Table I. High resolution INS measurements performed on IN5 with $\lambda = 6.7$ Å agree with the FDMRS results. Table I shows that while ferromagnetic exchange decreases in (ii), the d parameters actually increase. Again, nonaxial contributions to H are too small to be determined by these measurements, being a few percent of the axial ones. It is important to note that the present model reproduces the susceptibility measurements of both variants reported in [8,9].

Figure 3 clearly evidences that the giant-spin mapping completely breaks down in these two molecules, not only for the large S-mixing in the wave functions, but much more fundamentally for failing to account for the number of states located below the barrier. Since the main difference between (i) and (ii) is the position of the excited S manifolds, these systems provide the possibility to investigate the role of these manifolds in determining the relaxation dynamics. Many different relaxation paths passing through excited multiplets can contribute to the decay of M and it is not even obvious *a priori* that this decay should be monoexponential. To address this issue, we have calculated the relaxation dynamics of (i) and (ii) by master equations in which magnetoelastic (ME) coupling is modeled as in [12], i.e., with the quadrupole moments of each individual Mn ion isotropically coupled to Debye acoustic phonons.

This leads to transition rates W_{st} between pairs of eigenlevels of (1), given by

$$W_{st} = \gamma^2 \Delta_{st}^3 n(\Delta_{st}) \sum_{i,j,q_1,q_2} \langle s|O_{q_1,q_2}(\mathbf{s}_i)|t\rangle \overline{\langle s|O_{q_1,q_2}(\mathbf{s}_j)|t\rangle},$$

where i and j run over Mn ions, $O_{q_1,q_2}(\mathbf{s}_i)$ are the components of the Cartesian quadrupole tensor operator, $n(x) = (e^{\hbar x/k_B T} - 1)^{-1}$ and $\Delta_{st} = (E_s - E_t)/\hbar$. The advantage of this model is that it contains a single free parameter γ, proportional to the effective ME coupling strength. For both variants the resulting relaxation spectrum at low T is characterized by a *single* dominating relaxation time whose T-dependence displays a nearly Arrhenius behavior $\tau(T) = \tau_0 \exp(U/K_B T)$, in agreement with experiments [see the continuous lines in Fig. 1, calculated with $\gamma = 2.5 \times 10^{-3}$ THz^{-1} in (i) and 8.9×10^{-3} THz^{-1} in (ii)]. The reason underlying the presence of a single dominating time is essentially the same as in the conventional, giant-spin MNMs: in spite of multiplet nesting, the low-E levels continue to retain a two-well structure (Fig. 3)[13]. This leads to two separated time scales in the relaxation dynamics of M: Many fast intrawell processes producing internal equilibrium of each well, and a single very slow interwell process, governing the overall well-occupation probabilities [3]. If T and B are low enough that thermal fluctuations mainly result in unbalancing the relative population of the two wells, the regression of these fluctuations occurs through the slow process only, and single-time behavior results. With respect to a giant-spin MNM, the multistep processes connecting the two wells are here less obvious and the barrier U does not simply reflect the molecule's anisotropy. Indeed, U is an effective energy barrier which results from nontrivial weighted average of the energies of levels involved in the direct interwell transition paths. Thus, U is not determined by the ground-multiplet anisotropy alone, but by the mutual interplay of anisotropy and exchange. In fact, the large increase of the barrier of (i) with respect to (ii) results from the substantially larger exchange of the former variant. Indeed, by artificially isolating the ground $S = 12$ multiplet of (ii) the barrier reaches a value close to 100 K (see the dashed line in Fig. 1). It is important to stress that the value of the effective barrier is not set by the energy of the lowest-lying $M_S = 0$ eigenstate.

The nesting of different multiplets within the ground one implies that a magnetic field may induce crossings involving pairs of states belonging to different S manifolds. These are turned into anticrossings (acs) by the small nonaxial terms allowed by the low symmetry of the molecules. Such acs with the associated resonant incoherent tunneling, may result in additional steps in hysteresis cycles which are absent in a giant-spin MNM, where tunneling phenomena only involve the rotational dynamics of the giant-spin. In particular, the parameters of Table I imply that in addition to the giant-spin-type ac located at $B \sim 0.4$ T in both (i) and (ii) (involving states $|S = 12, M_S = 12\rangle$ and $|S = 12, M_S = -11\rangle$), other acs occur for small applied fields. The lowest-energy *intermultiplet* acs are: in (i) the ac involving $|S = 12, M_S = 11\rangle$ and $|S = 11, M_S = -11\rangle$ at $B \sim 0.3$ T; in (ii) the acs involving $|S = 12, M_S = 12\rangle$ and $|S = 11, M_S = -11\rangle$ at $B \sim 0.5$ T and $|S = 12, M_S = 11\rangle$ and $|S = 11, M_S = -11\rangle$ at $B \sim 0.1$ T. To check whether such tunneling processes are detectable, we show the numerical derivative of two measured $M(B)$ curves [8,9]. The results for two representative temperatures are shown in the insets of Fig. 3 together with the predicted positions. Peaks in dM/dB are clearly visible close to the predicted field values confirming the occurrence of intermultiplet tunneling in Mn_6.

In conclusion, by studying two different variants of Mn_6, we have investigated the role played by excited S multiplets that overlap with the ground one in the magnetic relaxation process. We have shown that a giant-spin picture is completely inappropriate for these systems because the effective energy barrier for the reversal of M crucially depends on the position of excited multiplets. Moreover, we have demonstrated the existence of tunneling pathways involving states of different total spin manifolds.

T. G. thanks M. Evangelisti for his useful suggestions.

[1] D. Gatteschi, R. Sessoli, and J. Villain, *Molecular Nanomagnets* (Oxford University, New York, 2006).
[2] W. Wernsdorfer and R. Sessoli, Science **284**, 133 (1999).
[3] P. Politi *et al.*, Phys. Rev. Lett. **75**, 537 (1995); A. Würger, J. Phys. Condens. Matter **10**, 10075 (1998); M. N. Leuenberger and D. Loss, Phys. Rev. B **61**, 1286 (2000); D. Zueco and J. L. Garcia-Palacios, Phys. Rev. B **73**, 104448 (2006).
[4] S. Carretta *et al.*, Phys. Rev. B **70**, 214403 (2004).
[5] S. Carretta *et al.*, Phys. Rev. Lett. **92**, 207205 (2004).
[6] A. Wilson *et al.*, Phys. Rev. B **74**, 140403 (2006).
[7] A. L. Barra *et al.*, J. Am. Chem. Soc. **129**, 10 754 (2007).
[8] C. J. Milios *et al.*, J. Am. Chem. Soc. **129**, 2754 (2007).
[9] C. J. Milios *et al.*, J. Am. Chem. Soc. **129**, 8 (2007).
[10] Because of S mixing, S is not a good quantum number. We label the states by their leading S component.
[11] The T dependence of high-energy peaks is partially hidden by the presence of phonons in the same energy range.
[12] S. Carretta *et al.*, Phys. Rev. Lett. **97**, 207201 (2006).
[13] Being the Hamiltonian almost axial, the z component of the total spin is conserved, even if S^2 is not. Thus, the selection rule $|\Delta M| \leq 2$ for phonon-induced transitions remains relevant and S mixing in the wave functions does not change the degree of separation of time scales of intra- and interwell processes (no interwell shortcuts are added by S mixing, unless resonant tunneling conditions occur).